Int. J. Electrochem. Sci., 6 **(2011)** 1396 - 1414

International Journal of
ELECTROCHEMICAL
SCIENCE
www.electrochemsci.org

Electrochemical, Thermodynamic and Adsorption Studies of (+)-Catechin Hydrate as Natural Mild Steel Corrosion Inhibitor in 1 M HCl

M. Hazwan Hussin[*] *and M. Jain Kassim*

Material and Corrosion Chemistry Laboratory, School of Chemical Sciences, Universiti Sains Malaysia, 11800, Penang, Malaysia.
[*]E-mail: mhh.km08@student.usm.my

Received: 9 March 2011 / *Accepted:* 23 April 2011 / *Published:* 1 May 2011

The inhibiting action of (+)-catechin hydrate on the corrosion of mild steel in hydrochloric acid has been studied. The results from weight loss, Tafel polarization and electrochemical impedance measurements consistently identify (+)-catechin hydrates as a good inhibitor. Polarization curves indicate that (+)-catechin hydrate act as mixed type inhibitor with predominant inhibition at anodic site. Impedance spectroscopy revealed that the corrosion of mild steel in hydrochloric solution was influenced to some extent by charge transfer. The inhibition efficiencies (IE %) of (+)-catechin hydrate was decreased exponentially with the temperatures. Surface analyses via scanning electron microscope (SEM) show a significant morphological improvement on the mild steel surface in addition of (+)-catechin hydrate. The inhibitive action of (+)-catechin hydrate follows the Langmuir adsorption model.

Keywords: A. metals, C. corrosion test, C. electrochemical techniques, D. corrosion.

1. INTRODUCTION

Catechin hydrate or known as taxifolin (Fig. 1) is a flavononol, a type of flavonoid. It can be found mostly in the Siberian larch (*Larix sibirica*) and in the silymarin extract from the milk thistle seeds. It's also found in small quantities in red onion. Catechin hydrate is not mutagenic and low toxic compared to other flavonoids [1]. It acts as a potential chemopreventive agent by regulating genes via ARE-dependent mechanism [2]. Due to high antioxidant activity, catechin hydrate has shown to inhibit the ovarian cancer cell growth [3], cellular melanogenesis [4], marine skin fibroblast and human breast cancer [5] in a dose-dependent manner. Despite all these, there is no study that has been done on the corrosion behavior of metals in the presence of catechin hydrate.

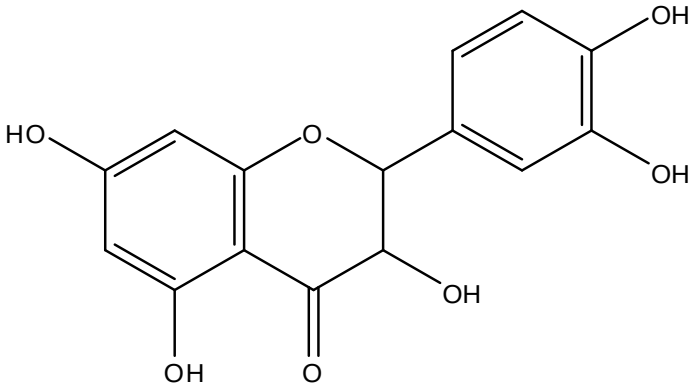

Figure 1. The structure of catechin hydrate.

Steel is highly susceptible to attack by acids. Hence for scale removal and cleaning of steel surfaces with acidic solutions, it becomes necessary to use inhibitors. In modern industry acids are used for the chemical cleaning of metals and alloys. Thus, to have inhibitors of the corrosion of these metals and alloys in acid solutions is not only beneficial but also at times indispensable. Most synthetic inhibitors are highly toxic [6] and thus leading to the investigations on the use of naturally occurring corrosion inhibitor [7-13] in the same time not harmful to both human and environment. Most of the potential corrosion inhibitor posses an active functional group such as nitro (-NO_2) and hydroxyl (-OH), heterocyclic compound and π electron [14-16]. Thus, the aim of this study is to evaluate the inhibitive effect of (+)-catechin hydrate as a natural corrosion inhibitor on the corrosion of mild steel in 1 M HCl solution. The assessment of the corrosion behavior was studied using weight loss and potentiodynamic polarization measurement, electrochemical impedance spectroscopy (EIS). Besides, the adsorption nature and surface morphology analysis using scanning electron microscope (SEM) was also determined.

2.MATERIAL AND METHODS

2.1. Materials

Standard (+)-catechin hydarate was purchased from Sigma Aldrich, USA. Mild steel coupons having chemical composition (wt %) of 0.08 C, 0.01 Si, 1.26 Mn, 0.02 P and remaining Fe were used. The specimens were polished successively using 400, 600 and 800 gritted emery papers. Next, it were degreased with methanol and washed with distilled water before and after experiment.

2.2. Electrolyte

The solutions used were made of AR grade hydrochloric acid. Appropriate concentrations of acids were prepared by using distilled water. The concentration range of (+)-catechin hydrate standard

employed varied from 100 ppm to 5000 ppm for the effect of concentration, while for the effect of temperature, the range was from 250 ppm to 1000 ppm in deaerated solution.

2.3. Weight loss method

Weight loss of rectangular mild steel specimens with dimension of 3 cm x 4 cm x 0.1 cm were determined in 100 mL of electrolyte with and without the addition of different concentrations of standard (+)-catechin hydrate were determined after 24 hours at room temperature. The percentage inhibition efficiency (IE) was calculated from,

$$IE\ \% = \frac{W_o - W'}{W_o} \times 100 \quad (1)$$

where W_o and W' are the weight loss values in absence and in presence of inhibitor and to calculate the corrosion rate R_{corr} of mild steel, the following equation is used:

$$R_{corr}\ (mpy) = \frac{534\ W}{\rho A t} \quad (2)$$

where W is the weight loss (mg), ρ is the density of mild steel (7.8 g cm^{-3}), A is the area of specimen (4.7244 in^2) and t is the time of immersion (24 hr). The general unit for the corrosion rate is in mpy or mils (0.001 in) of penetration per year.

2.5. Electrochemical measurements

A three electrode cell assembly consisting of a mild steel coupon of the size 6 cm x 4 cm x 1 mm dimension as working electrode (WE) with an exposure surface of 0.78 cm^2, platinum rod as counter electrode (CE) and saturated calomel electrode (SCE) as reference electrode (RE) containing 300 mL of electrolyte were used for electrochemical measurement. The temperature of the electrolyte was maintained at room temperature (30 °C).

2.6. Potentiodynamic Polarization

Potentiodynamic polarization studies were carried out using VoltaLab Potentiostat (Model PGP201) at room temperature without and with addition of various concentrations of 1 M HCl solutions of inhibitors (0, 100, 500, 1000, 2000, 3000, 5000 ppm) at a scan rate of 1 mVs^{-1}. Open circuit potential $E_{ocp,}$ was measured for 30 minutes to allow stabilization of the steady state potential. The potential range was scanned from the E_{ocp} values obtained (± 250 mV). The inhibition efficiency IE was calculated by using the following equation,

$$IE\ \% = \frac{I_{corr} - I_{corr}'}{I_{corr}} \times 100 \quad (3)$$

where I_{corr} and I_{corr}' are referred to corrosion current density without and with addition of (+)-catechin hydrate in mA cm^{-2} respectively. Potentiodynamic polarization curves were produced using Volta Master 4 software.

2.7. Electrochemical Impedance Spectroscopy (EIS)

The electrochemical impedance spectroscopy (EIS), was carried out using Gamry Instrument Reference600 with the open circuit potential, E_{ocp} of every samples was immersed for 30 min over a frequency range of 100 kHz to 0.01 Hz with a signal amplitude perturbation of 5 mV and scan rate of 1 mVs^{-1}. Next, it was fitted with sets of circuit using Echem Analyst software that give the best value. The inhibition efficiency IE was calculated by the following equations,

$$IE\ \% = \left(1 - \frac{R_{ct}}{R_{ct}'}\right) \times 100 \quad (4)$$

where R_{ct} and R_{ct}' are referred to charge transfer resistance without and with addition of (+)-catechin hydrate in Ω cm^2 respectively.

2.8. Surface adsorption and morphology analysis

The surface adsorption nature of mild steel was further understood by employing potential zero charge (PZC) analysis where the optimum concentration of (+)-catechin hydrate was determined using Gamry Instrument Reference600 AC Voltametry. The maximum frequency (f_{max}) of each samples were first identified from Bode plot. The initial and final potential range was set at -1 V to 1 V with voltage step value of 0.01. The surface morphology of steels specimens were evaluated by scanning electron microscope (SEM) analysis (Leo Supra 50VP). A test specimen that exhibit higher efficiency of corrosion inhibition from weight loss measurement was examined with scanning electron microscopy (SEM) instead of blank (without inhibitor) and fresh steel.

3. RESULTS AND DISCUSSION

3.1. Effect of concentration

3.1.1. Weight loss measurement

Table 1 show the inhibition efficiency of mild steel with and without the addition of different concentrations of (+)-catechin hydrate determined after 24 hours at room temperature. It has been

observed that 1000 ppm of (+)-catechin hydrate works as an optimum concentration of corrosion inhibition. The results indicated that (+)-catechin hydrate is concentration-independent with the inhibition efficiency where a slight decrease is observed at higher concentration (Fig. 2).

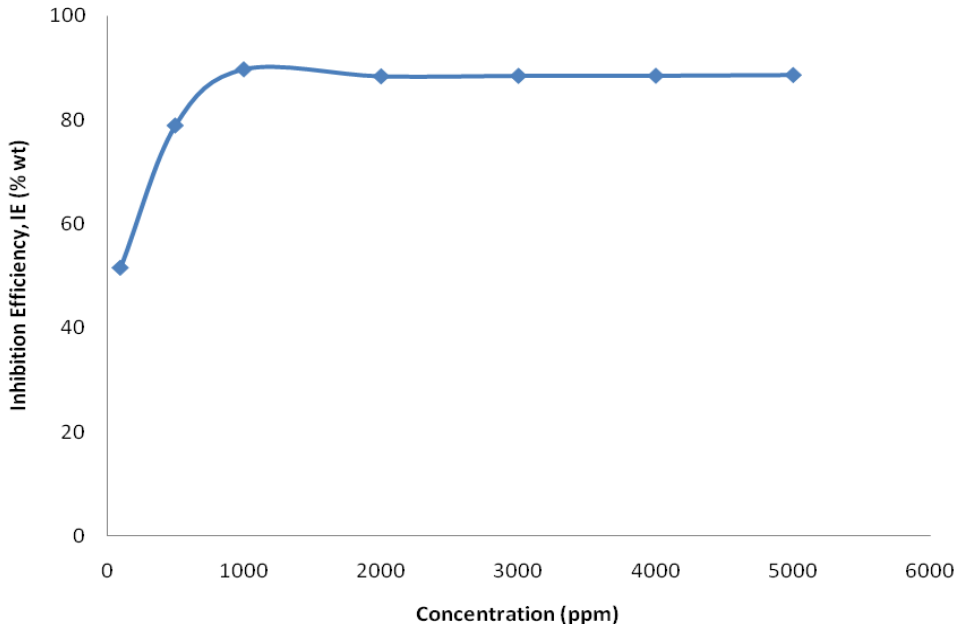

Figure 2. The relation between percentage of inhibition with concentration of (+)-catechin hydrate.

Table 1. Effect of inhibitor concentration on inhibitor efficiency of (+)-catechin hydrate in 1 M HCl.

Conc. (ppm)	Weight loss (g)	IE (wt %)	R_{corr} (mpy)
0	2.0134	-	2.2765
100	0.9769	51.48	1.1046
500	0.4242	78.93	0.4796
1000	0.2059	89.77	0.2328
2000	0.2332	88.42	0.2637
3000	0.2313	88.51	0.2615
5000	0.2281	88.67	0.2579

The corrosion rate of mild steel decreased on increasing the inhibitor concentration (until 1000 ppm). This behaviour could be attributed to the increase in adsorption of inhibitor at the metal/solution interface on increasing its concentration. An increase of inhibitor concentration beyond 1000 ppm resulted in a diminished corrosion protection. This may be due to the withdrawal of adsorbate (inhibitor) back into the bulk solution when the concentration of inhibitor closed to or beyond the critical concentration [17]. The above effect leads to the weakening of metal-inhibitor interactions, resulting in the replacement of inhibitor by water or chloride ions (Cl^-) with decrease in inhibition efficiency [18]. Interestingly, the color of working electrode consisting (+)-catechin hydrate were

changed to a dark blue complex which indicated the formation of a stable magnetite on the mild steel. The magnetite was strongly adhere to the metal surface and consequently results an impermeable layer to stop further corrosion process [19, 20].

3.1.2. Potentiodynamic Polarization measurement

Fig. 3 represents the anodic and cathodic Tafel polarization curves of mild steel in different concentration of 1 M HCl solutions of (+)-catechin hydrate. By extrapolating the Tafel anodic and cathodic linear parts until they intersect as straight lines and show the corrosion current density (I_{corr}) and corrosion potential (E_{corr}) as well as polarization resistance (R_p). A steady state of corrosion current density (I_{corr}) occurs when the measured curve becomes horizontal [21]. The inhibition of these reactions was more pronounced on increasing inhibitor concentration until 1000 ppm where the efficiency starts to decrease and arise back.

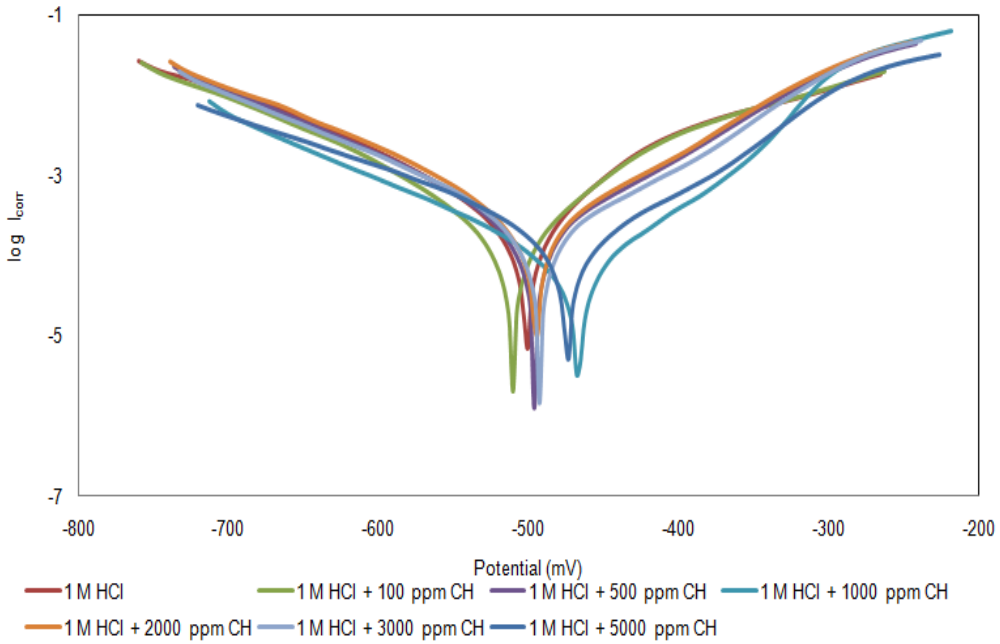

Figure 3. Tafel curve for mild steel in 1 M HCl solution in absence and presence of (+)-catechin hydrate.

Increasing the inhibitor concentration will decrease the corrosion current densities [22, 23]. According to Ahamad *et al.* (2010), this is may be due to the adsorption of the inhibitor on mild steel/acid solution interface [23]. Here, it shows that the decrease of current density of all inhibitors in comparison with 1 M HCl for both anodic and cathodic site may suggest the mixed type of corrosion inhibition behavior with predominant decrease at anodic site. Basically, anodic polarization is the shift of anode potential to the positive (noble) direction whereas cathodic polarization is the shift of cathode potential to the negative (active) direction.

Table 2: The polarization parameter values for the corrosion of mild steel in 1 M HCl solution containing different concentrations of (+)-catechin hydrate.

Concentration (ppm)	E_{corr}, (mV)	I_{corr}, (mA cm^{-2})	R_p, (Ω cm^2)	β_a (mV)	$-\beta_c$ (mV)	R_{Corr}, (mm y^{-1})	IE (%)
0	-505	0.2158	86.29	78.4	100.6	2.523	-
100	-518	0.2042	86.31	112.7	130.9	2.478	5.38
500	-504	0.1653	99.60	95.6	93.3	1.933	23.40
1000	-475	0.0591	269.72	82.0	102.7	0.691	72.60
2000	-501	0.1630	96.60	99.0	94.9	2.324	17.92
3000	-500	0.1491	108.86	100.3	93.8	1.744	30.58
5000	-480	0.1088	157.86	99.5	105.5	1.272	49.58

In literature [17, 23], it has been reported that if the displacement in E_{corr} is >85 mV the inhibitor can be seen as a cathodic or anodic type inhibitor and if the displacement of E_{corr} is <85 mV, the inhibitor can be seen as mixed type. In this study, the maximum displacement in E_{corr} value was 30 mV for inhibitors which indicates that the inhibitors act as mixed type inhibitor with predominant anodic effectiveness. A study of corrosion prevention and protection have supported that mixed type of inhibitors are generally represented by organic compounds with donor atoms Se, S, N or O instead of having reactive functional groups which latch on to the metal [24]. For this reason, it was comfirmed by potentiodynamic polarization curve that (+)-catechin hydrate exhibits a mixed-type inhibitor with the highest efficiency at 1000 ppm. Electrochemical corrosion parameters obtained from the Tafel analysis of the polarization curve from Fig. 3 were illustrated in Table 2.

3.1.3. Electrochemical Impedance Spectroscopy

The corrosion of mild steel in 1 M HCl solution were investigate using EIS at room temperature after an exposure period of 30 min. Nyquist plots for mild steel obtained at the interface in the absence and presence of (+)-catechin hydrate at different concentrations is given in Fig. 4. The impedance diagram obtained with 1 M HCl shows only one depressed capacitive loop at the higher frequency range.

The same trend was also noticed for mild steel immersed in 1 M HCl containing inhibitors (100-5000 ppm). This indicates that the corrosion of mild steel in the absence and presence of the inhibitors is mainly controlled by a charge transfer process [13]. Table 3 lists the impedance parameters of Nyquist plots at different concentrations.

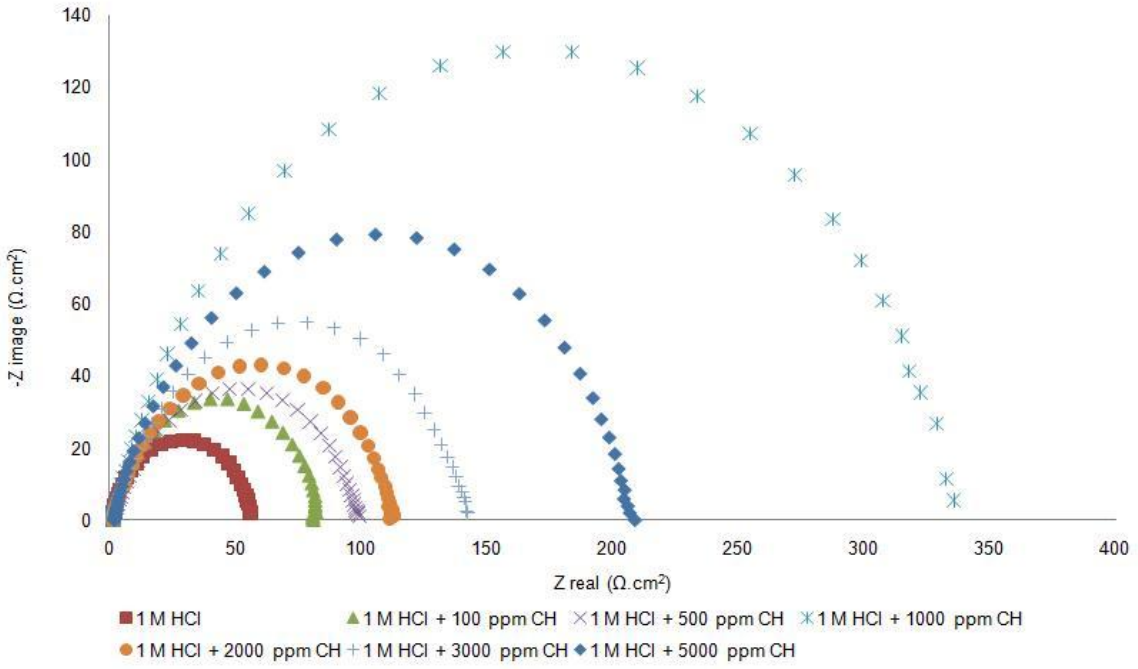

Figure 4. Nyquist plot for mild steel in 1 M HCl solution in presence of (+)-catechin hydrate.

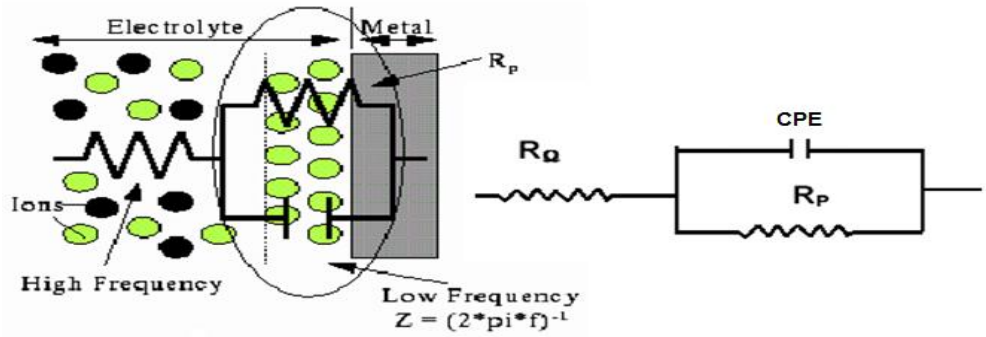

Figure 5. The Randles CPE circuit which is the equivalent circuit for this impedance spectra.

Table 3. Impedance parameters and inhibition efficiency for mild steel in 1 M HCl solutions containing different concentrations of (+)-catechin hydrate

Concentration (ppm)	R_{ct} (Ω cm^2)	R_s (Ω cm^2)	CPE (μF cm^{-2})	n	% IE
0	40.02	1.213	939.8	0.7149	-
100	64.81	0.903	461.7	0.8029	32.25
500	78.37	0.977	258.5	0.8122	48.93
1000	269.3	0.986	154.9	0.8601	85.14
2000	89.26	1.038	390.1	0.8012	55.16
3000	113.4	1.186	361.8	0.8029	64.71
5000	206.7	1.196	213.5	0.8381	80.31

R_{ct} represents the charge-transfer resistance whose value is a measure of electron transfer across the surface and is inversely proportional to corrosion rate [25]. The constant phase element, CPE (Fig. 5), is introduced in the circuit instead of a pure double layer capacitor to give a more accurate fit [26].

The diameter of Nyquist plots increases on increasing the inhibitors concentration. This suggested that the formed inhibitive film was strengthened by addition of inhibitors. The high frequency (HF) loops have depressed semicircular appearance, $0.5 \leq n \leq 1$, which is often referred to as frequency dispersion as a result of the inhomogeneity [27-29] or the roughness [30] of the solid surface.

Besides, the presence of low frequency (LF) inductive maybe attributed to the relaxation process obtained by adsorption species like Cl^{-1}_{ads} and H^{+}_{ads} on the electrode surface. It may also attribute to the re-dissolution of the passivated surface at low frequency (LF) [23]. It should be noted that a CPE (Fig. 5) could be treated as a parallel combination of a pure capacitor and a resistor being inversely proportional to the angular frequency. The CPE, which is considered a surface irregularity of the electrode, causes a greater depression in Nyquist semicircle diagram, where the metal-solution interface acts as a capacitor with irregular surface [17]. The impedance of the CPE is expressed as:

$$Z_{CPE} = \frac{1}{Y_0(j\omega)^n} \quad (5)$$

where Y_0 is the magnitude of the CPE, j is the imaginary unit, ω is the angular frequency ($\omega = 2\pi f$, where f is the AC frequency) and n is the CPE exponent (phase shift). The general unit for CPE is in F cm^{-2} (Farad cm^{-2}). The EIS measurement reveals that at the concentration of 1000 ppm, the percentage of inhibition efficiency is highest. The result strongly supports the observation that 1000 ppm of (+)-catechin hydrate could work best as an inhibitor.

3.2. Effect of temperature

Generally, the corrosion rate of mild steel in acidic solution increase with the rise of temperature. This is due to the decrease of hydrogen evolution overpotential [31]. In order to understand more about the performance of (+)-catechin hydrate with the nature of adsorption and activation processes, the effect of temperature is studied.

For this purpose, the weight loss measurements are being employed with the range of temperature 303, 313, 323 and 333 K for 24 hr of immersion.

From the Arrhenius plots obtained, the activation energy (E_a) can be calculated and thus further explanations on the mechanism of the inhibitive process can be discussed [32]. The degree of surface coverage θ for different concentrations of (+)-catechin hydrate has been evaluated using the equation:

$$\theta = \frac{W_0 - W'}{W_0 - W_m} \quad (6)$$

where W_0 and W' are the weight loss values in absence and in presence of inhibitor. W_m is the smallest corrosion rate. Table 4 summarized the corresponding efficiency at various temperatures. As (+)-catechin hydrate has been added into the solution, the degree of surface coverage values decreases slightly with increasing temperature in which it could be caused by the desorption of inhibitor from the mild steel surface.

Table 4. Effect of temperature on the mild steel corrosion in 1 M HCl for various concentrations of (+)-catechin hydrate.

Temperature (K)	Concentration (ppm)	W_0/W' (g)	W (mg cm^{-2} h^{-1})	IE (wt %)	θ	θ/1-θ
303	0	0.2279	0.7913	-	-	-
	250	0.1137	0.3948	50.11	0.5011	1.0044
	500	0.0535	0.1858	76.52	0.7652	3.2589
	750	0.0349	0.1212	84.69	0.8469	5.5317
	1000	0.0244	0.0847	89.28	0.8928	8.3284
313	0	0.6053	2.1017	-	-	-
	250	0.3912	1.3583	35.37	0.3537	0.5473
	500	0.1738	0.6035	71.29	0.7129	2.4831
	750	0.1027	0.3566	83.03	0.8303	4.8928
	1000	0.0687	0.2385	88.64	0.8864	7.8028
323	0	1.925	6.6840	-	-	-
	250	1.3338	4.6313	30.71	0.3071	0.4432
	500	0.9137	3.1726	52.54	0.5254	1.1070
	750	0.791	2.7465	58.91	0.5891	1.4337
	1000	0.5842	2.0285	69.65	0.6965	2.2948
333	0	2.7169	9.4337	-	-	-
	250	2.7147	9.4260	0.809	0.0008	0.0008
	500	2.2873	7.9420	15.81	0.1581	0.1878
	750	2.1681	7.5281	20.19	0.2019	0.2529
	1000	1.6614	5.7688	38.85	0.3885	0.6353

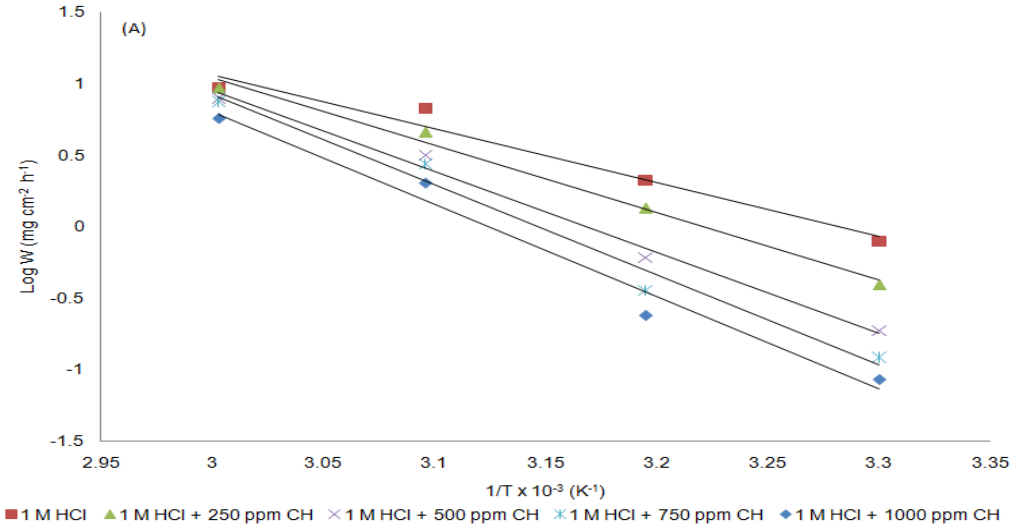

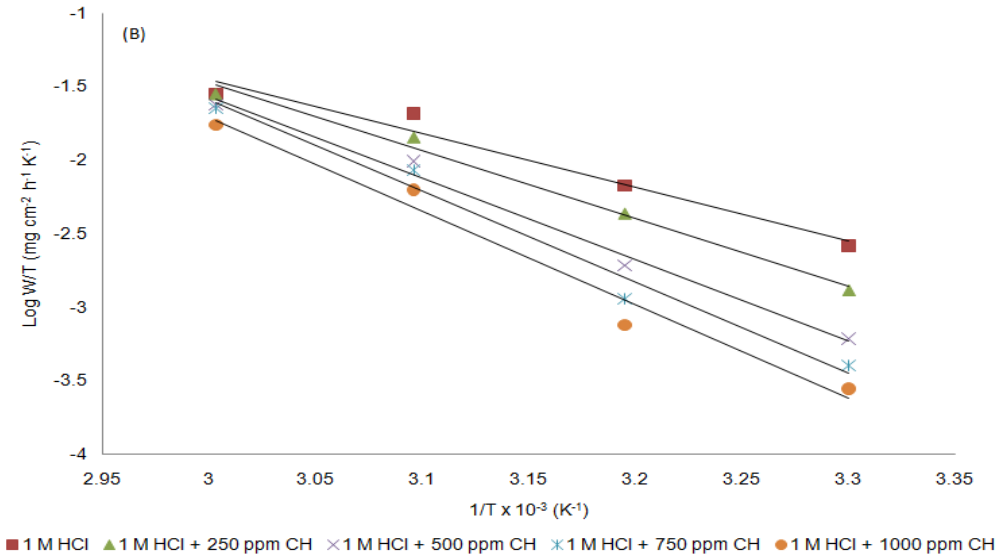

Figure 6. (A) Arrhenius plots and (B) Transition state plots for mild steel in 1 M HCl at different concentration of (+)-catechin hydrate.

In order to calculate activation thermodynamic parameters of the corrosion reaction such as activation energy E_a, activated entropy ΔS and enthalpy ΔH, the Arrhenius equation and its alternative formulation called transition state equation were employed [33]:

$$W = K\,exp\left(-\frac{E_a}{RT}\right) \tag{7}$$

$$W = \frac{RT}{Nh}exp\left(\frac{\Delta S}{R}\right)exp\left(-\frac{\Delta H}{RT}\right) \tag{8}$$

T is the absolute temperature, K is a constant and R is the universal gas constant, h is Plank's constant, N is Avogadro's number. The activation energy can be calculated from the slope ($-E_a/2.303R$) by plotting the logarithm of corrosion rate versus $1/T$.

Fig. 6A shows the variations of logarithm of the corrosion rate with the presence and absence of inhibitor with the reciprocal of absolute temperature.

The activation energies in the presence of (+)-catechin hydrate were observed higher than those in absence of (+)-catechin hydrate (Table 5). This explains that the energy barrier of corrosion reaction increases with the concentration of (+)-catechin hydrate. In addition, the value of activation energy that is around 40 to 80 kJ mol^{-1} can be suggested to obey the physical adsorption (physiosorption) mechanism [34]. Physiosorption is often related with this phenomenon, where an adsorptive film of electrostatic character is formed on the mild steel surface [31]. In addition, high value of activation energy will lower the corrosion rate or lower the corrosion current density. This indicates that the electron transfer in oxidation-reduction processes will become less dense and hence lower the corrosion rate [35].

Table 5. Activation parameters of the dissolution reaction of mild steel in 1 M HCl in the absence and presence of (+)-catechin hydrate.

Concentration (ppm)	E_a (kJ mol^{-1})	-ΔH (kJ mol^{-1})	ΔS (J $mol^{-1}K^{-1}$)
0	22.0902	20.9429	-35.24
250	39.2769	38.1313	16.31
500	47.1612	46.0172	39.23
750	52.5994	51.4537	55.31
1000	53.9495	52.8030	58.35

The thermodynamic parameters (Δ*S* and Δ*H*) calculated from the linear regression of transition state (Fig. 6B), show that the dissolution reaction of mild steel in 1 M HCl in the presence of (+)-catechin hydrate are higher than in absence of (+)-catechin hydrate (Table 5). Positive value of activated enthalpy, Δ*H* means that the process is an exothermic process and it needs more energy to achieve the activated state or equilibrium state [33, 35]. Also, the positive of activated entropy, Δ*S* of solution containing (+)-catechin hydrate indicates that the system passes from less orderly to a more random arrangement [36].

3.3. Adsorption Isotherm

The adsorption process of inhibitor is a displacement reaction where the adsorbed water molecule is being removed from the surface of metal [37]:

$$Org\ (sol) + nH_2O\ (ads) \rightarrow Org\ (ads) + nH_2O\ (sol)$$

Org(sol) and *Org(ads)* are the organic molecules in the aqueous solution that adsorbed to the metal surface. While $H_2O(ads)$ is the water molecule on the metal surface in which *n* is the coefficient that represent water molecules replaced by a unit of (+)-catechin hydrate. To obtain an effective adsorption of an inhibitor on metal surface, the interaction force between metal and inhibitor must be greater than the interaction force of metal and water molecule [24]. The corrosion adsorption processes can be understood using adsorption isotherm. Langmuir adsorption isotherm is attributing to physisorption or chemisorption phenomenon while Temkin adsorption isotherm gives an explanation about the heterogeneity formed on the metal surface. Chemisorption is attributed to Temkin isotherm [36]. Here, Langmuir, Frumkin and Temkin adsorption isotherm were applied in order to explain the adsorption process of (+)-catechin hydrate on the mild steel surface:

Langmuir: $C/\theta = 1/K + C$ (9)

Frumkin: $\log \{\theta/(1-\theta)\ C\} = \log K + g\theta$ (10)

Temkin: $log\ (\theta/C) = log\ K - g\theta$ (11)

θ is the surface coverage, K is the adsorption-desorption equilibrium constant, C is the concentration of inhibitor and g is the adsorbate parameter. Again, the weight loss measurements were employed in this experiment with the concentration range 250, 500, 750 and 1000 ppm at 303 K. The corresponding plots are shown in Fig. 7, where the r^2 value for Langmuir isotherm (Fig. 7A) was 0.9915, Frumkin isotherm (Fig. 7B) was 0.9981 and Temkin isotherm (Fig. 7C) was 0.8564. From this observation, it is concluded that Langmuir isotherm shows the best correlation with the experimental data. In addition, this also explains the monolayer formation of the inhibitor onto the mild steel surface [35, 37]. The free energy of adsorption ΔG_{ads}, also can be calculated using the following equation:

$$\Delta G_{ads} = -RT\ ln(K \times 55.5) \quad (12)$$

where 55.5 is the molar concentration of water, R is the universal gas constant and T is the temperature in K. The calculated value of free energy of adsorption was found to be ΔG_{ads} = -13.4570 kJ mol^{-1}, where adsorption-desorption equilibrium constant K value was obtained from the linear regression of Langmuir isotherm (3.7651 M^{-1}).

The negative value of ΔG_{ads} indicates that the inhibitor, in this case (+)-catechin hydrate is spontaneously adsorbed onto the mild steel surface. It is well known that values of ΔG_{ads} around -20 kJ mol^{-1} or lower are associated with the physiosorption phenomenon where the electrostatic interaction assemble between the charged molecule and the charged metal, while those around -40 kJ mol^{-1} or higher are associated with the chemiosorption phenomenon where the sharing or transfer of organic molecules charge with the metal surface occurs [38, 39].

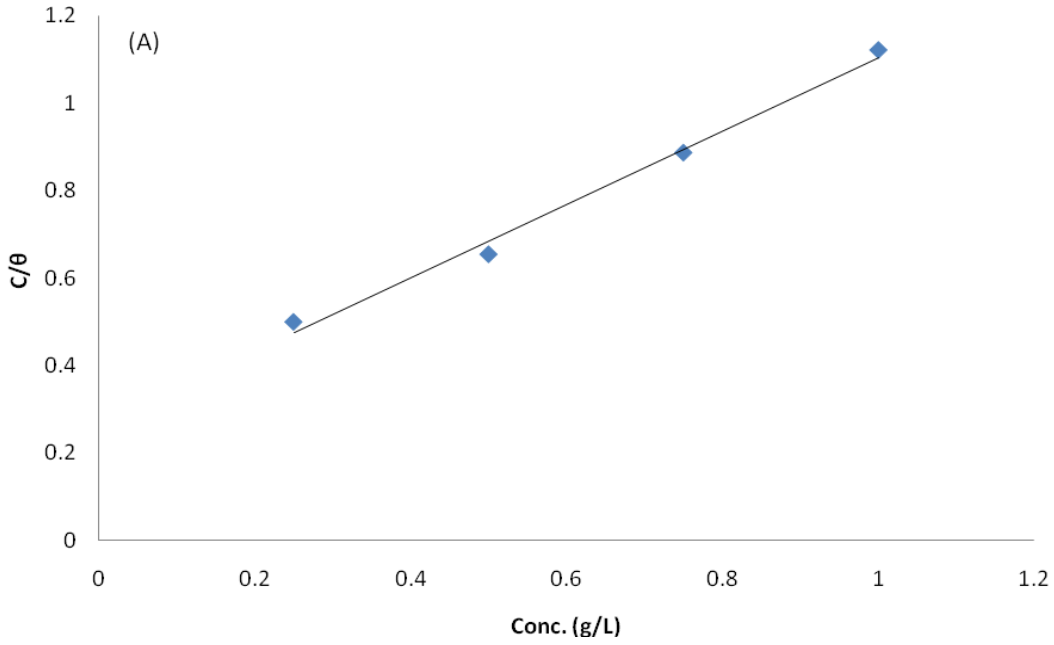

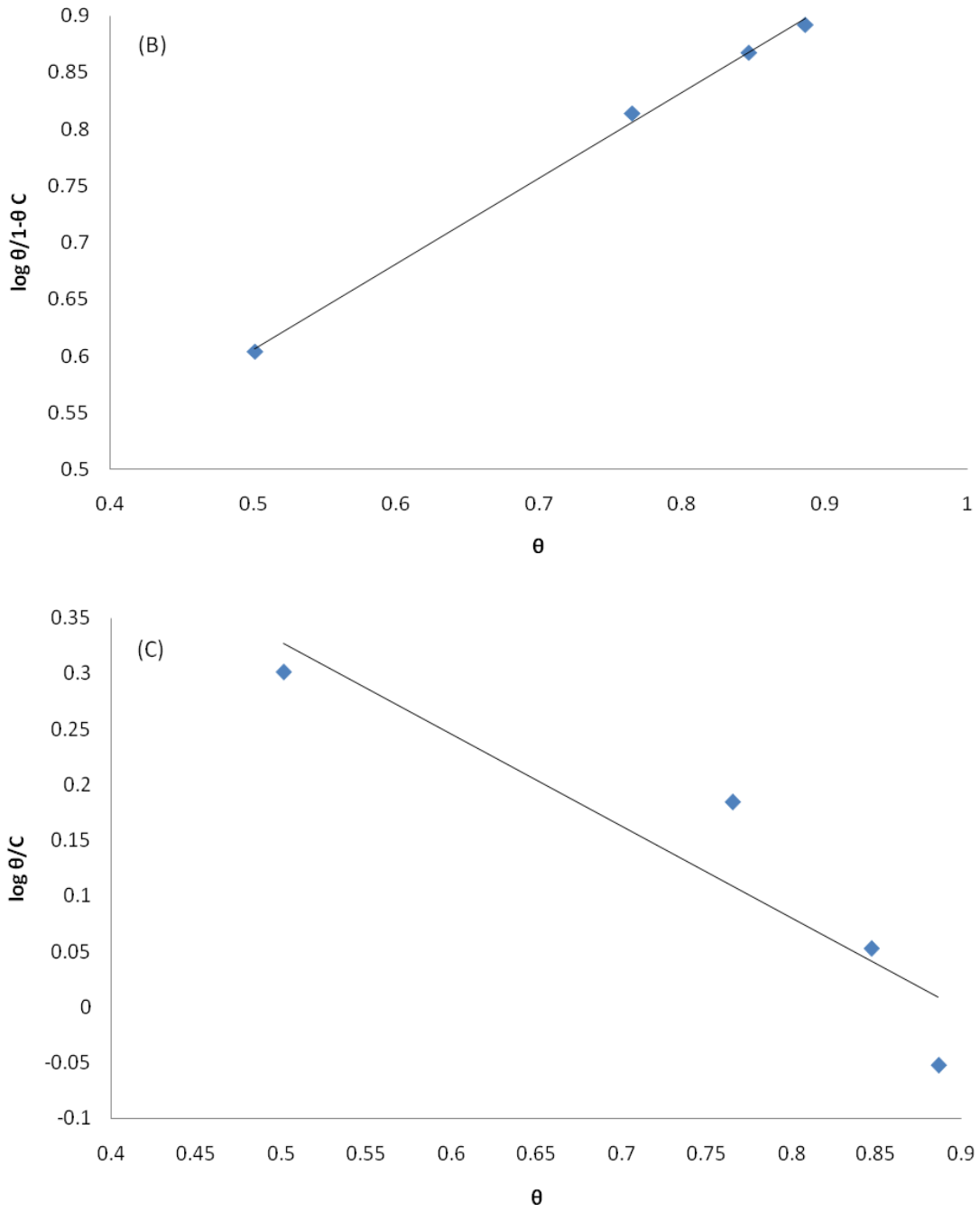

Figure 7. (A) Langmuir, (B) Frumkin and (C) Temkin isotherm for the adsorption of (+)-catechin hydrate on the surface of mild steel in 1 M HCl.

Hence, it is clear that (+)-catechin hydrate is physically adsorbed onto the mild steel surface. Moreover, the exponential correlation between inhibition efficiency with temperature may supports that the adsorption of (+)-catechin hydrate on the mild steel surface is physical in nature. As the temperature increases, the number of adsorbed molecules decreases, leading to a decrease in the inhibition efficiency. The adsorption is enhanced by the presence of electron donor atom of O, with lone pair electron and delocalized π electrons in the (+)-catechin hydrate molecules that create

electrostatic adsortion with the mild steel surface. As a result, insoluble stable films formed on the mild steel surface thus decrease the metal dissolution.

3.4. Surface adsorption and morphology analysis

The adsorption process was affected by the chemical structures of the inhibitors, the nature and charged surface of the metal and the distribution of charge over the whole inhibitor molecule.

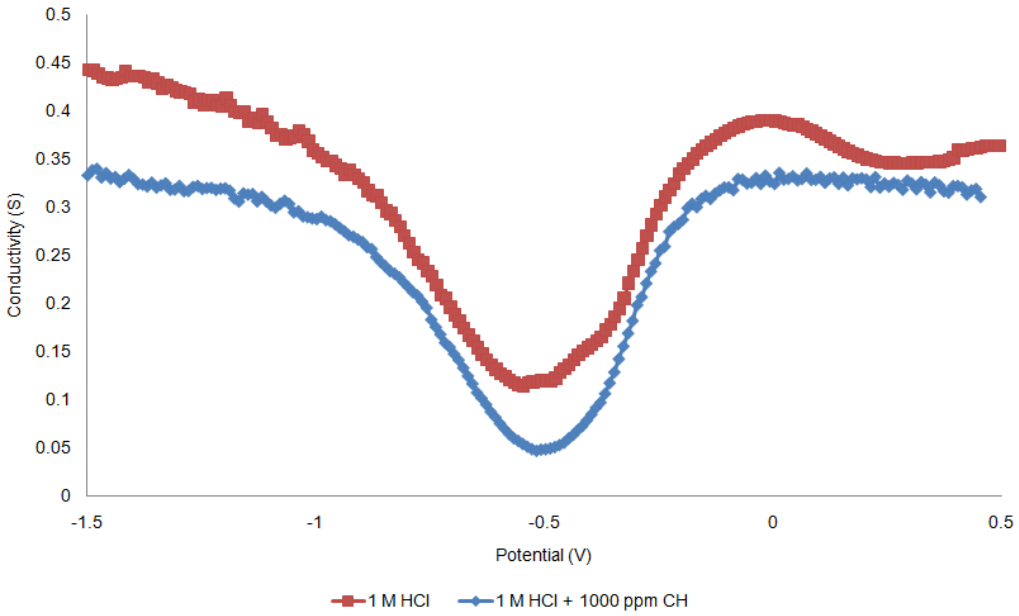

Figure 8. Relation between conductivity and the applied potential on a steel electrode immersed in 1 M HCl without and with (+)-catechin hydrate.

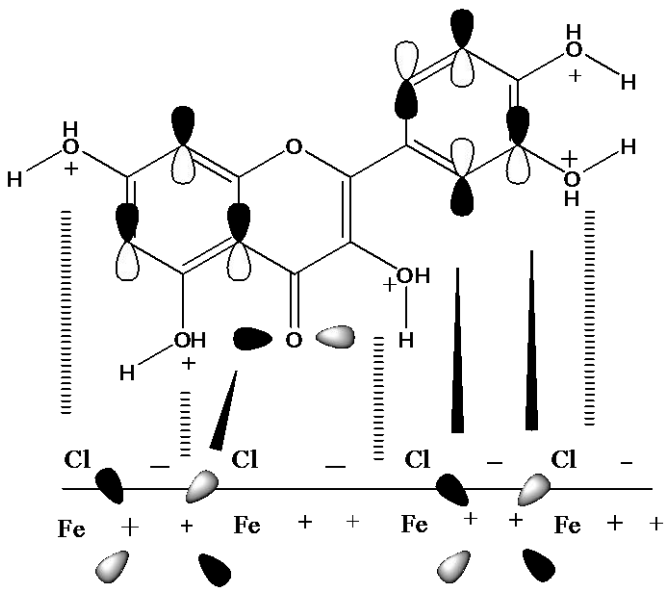

Figure 9. The schematic illustration of different modes of adsorption on mild steel/1 M HCl interface.

The potential zero charge (PZC) may help in determining the type of adsorption that occurs at the electrode surface [40]. The electrochemical impedance spectroscopy (EIS) offers a good method in order to determine the PZC of metal [41]. When the difference of $E_r = E_{corr} - PZC$ was negative, where E_r is the Antropov 'rational' corrosion potential, the working electrode surface has a negative net charge and the adsorption of cations was favoured. On contrary, adsorption of anions was favoured when E_r become positive. The different charge of metals under conditions of their corrosion might be considered as one of the reasons for the selective action of inhibitors [42]. Thus, the PZC of mild steel must be calculated in studied conditions to explain the inhibiting action of inhibitors (Table 6). The values of PZC obtained are more negative than the corrosion potential E_{corr} values. This is due to the change of the discharge surface of mild steel in acidic solution [43].

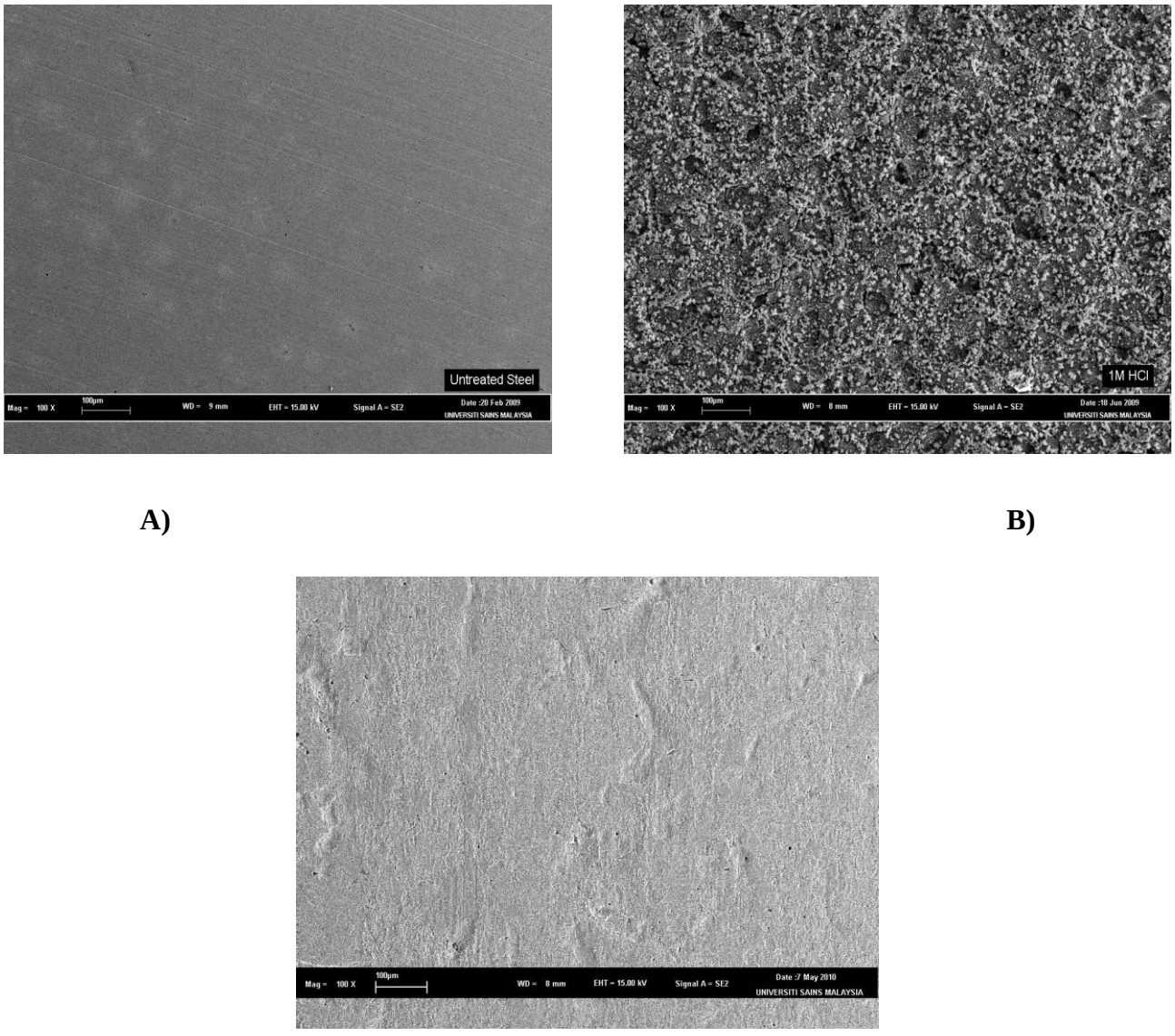

Figure 10. SEM micrographs of: a) mild steel, b) mild steel without inhibitor, 0 ppm, c) mild steel with (+)-catechin hydrate, 1000 ppm at magnification of 100 x.

The corresponding plot (Fig. 8) shows the correlation between conductivity (in Siemens) with potential. Conductivity is the reciprocal (inverse) of resistivity. EIS analysis has shown that in the presence of the inhibitor, the charge transfer resistance value R_{ct}, will be higher whereas in the absence of the inhibitor, R_{ct} value will be lower. Thus, in the presence of the inhibitor, the conductivity values should be lower than in absence on the inhibitor [44]. In the presence of optimum concentration of 1000 ppm (+)-catechin hydrate in 1 M HCl solution, the conductivity seems to be lower than in absence of both inhibitors. Positive value of E_r indicated that the positively charged mild steel will be specifically adsorbed by chloride ions (anions).

Table 6. Values of E_r for the mild steel electrode in 1 M HCl for (+)-catechin hydrate.

Sample	f_{max} (Hz)	E_{corr} (mV)	PZC (mV)	E_r (mV)
1 M HCl	253	-505	-545	40
1 M HCl + 1000 ppm (+)-catechin hydrate	199	-484	-518	34

The adsorption of negatively charged chloride ions on the mild steel surface creates an excess negative charge on the surface thus leading to adsorption of cations (protonated inhibitors). The protonated inhibitor molecules will adsorb on the mild steel surface via chloride ions which form an interconnecting bridge between positively charged mild steel surface and protonated inhibitors [41]. Electrostatic interaction was believed to occur between the protonated molecules and $(FeCl^-)_{ads}$ species at anodic sites (Fig. 9). Potentiodynamic polarization measurement have proved that the inhibition of both inhibitors were predominately at the anodic site. Surface analysis using scanning electron microscope (SEM) proved a significant morphological improvement on the surface of mild steel plates in the presence of (+)-catechin hydrate. From Fig. 10B, a rough surface was noticed for mild steel immersed in 1 M HCl solution. On the other hand, a smooth surface was observed in the inhibited mild steel surface (Fig. 10C) and it is comparable with the polished surface (Fig. 10A).

4. CONCLUSIONS

- The (+)-catechin hydrate shows good corrosion inhibition properties for mild steel in 1 M HCl. The comparative study by means of inhibition efficiency for all electrochemical tests and weight loss measurements were in good agreement at the concentration of 1000 ppm.
- Potentiondynamic polarization measurements demonstrate that (+)-catechin hyrdrate acts as a mixed-type inhibition with anodic as its dominant. Electrochemical impedance spectroscopy (EIS) revealed that the corrosion of mild steel in the absence and presence of the inhibitors was mainly controlled by a charge transfer process.

- The adsorption of (+)-catechin hydrate on the mild steel surface follows the Langmuir adsorption isotherm. From the free energy of adsorption ΔG_{ads} values, it can be concluded that the adsorption process was spontaneous and physically adsorbed (physiosorption) onto the mild steel surface.
- Surface analysis show that there were tremendous morphological improvements on the mild steel surface after being added with (+)-catechin hydrate.

ACKNOWLEDGEMENT
The authors would like to thank the Universiti Sains Malaysia for the financial support given through the USM Short Term Grant Scheme (304/PKIMIA/635055) and the RU-USM-Postgraduate Research Grant Scheme (1001/PKIMIA/831016).

References

1. P.S. Makena, S.C. Pierce, K.T. Chung, S.E. Sinclair, *Environmental and Molecular Mutagenesis* 50 (6) (2009) 451.
2. S.B. Lee, K.H. Cha, D. Selenge, A. Solongo, C.W. Nho, *Biological & Pharmaceutical Bulletin* 30 (2007) 1074.
3. H. Luo, B.H. Jiang, S. King, Y.C. Chen, *Nutrition and Cancer* 60 (6) (2008) 800.
4. Y.S. Tarahovsky, I.I. Selezneva, N.A. Vasilieva, M.A. Egorochkin, Y.A. Kim, *Bulletin of Experimental Biology and Medicine* 144 (6) (2007) 791.
5. V.S Rogovskii, A.I. Matiushin, N.L. Shimanovskii, A.V. Semeikin, T.S. Kukhareva, A.M. Koroteev, M.P. Koroteev, E*ksperimental'naia i klinicheskaia farmakologiia* 73 (9) (2010) 39.
6. A.Ostovari, S. M. Hoseinieh, M. Peikari, S. R. Shadizadeh, S. J. Hashemi, *Corros. Sci.* 51 (2009) 1935–1949.
7. L. Valek, S. Martinez, *Mater. Lett*. 61 (2007) 148.
8. I. Radojcic, K. Berkovic, S. Kovac, J. Vorkapic-Furac, *Corros. Sci*. 50 (2008) 1498.
9. A.Y. El-Etre, *App. Surf. Sci*. 252 (2006) 8521.
10. K.O. Orubite, N.C. Oforka, *Mater. Lett*. 58 (2004) 1768.
11. E.E. Oguzie, *Corros. Sci*. 49 (2007) 1527.
12. A.A. Rahim, E. Rocca, J. Steinmetz, M. Jain Kassim, *Corros. Sci*. 50 (2008) 1546.
13. M. H. Hussin, and M. J. Kassim, *Mater. Chem. Phys*. 125 (2011) 461-468.
14. J.R. Davis, Corrosion: Understanding The Basic, ASM International, The Materials Information Society, Ohio, 2000.
15. P.A. Schweitzer, Corrosion of Linings and Coatings, Cathodic and Inhibition Protection and Corrosion Monitering, Taylor & Francis Group, New York, 2007.
16. R.W. Revie, H.H. Uhlig, Corrosion and Corrosion Control: An Introduction to Corrosion Science and Engineering, 4th Edition, John Wiley & Sons Ltd., New Jersey, 2008.
17. A.K. Satapathy, G. Gunasekaran, S. C. Sahoo, Kumar Amit, P. V. Rodrigues, *Corros. Sci*. 51 (2009), 2848–2856.
18. G. Gunasekaran, L. R. Chauhan, *Electrochim. Acta* 49 (2004), 4387.
19. O. Lahodry-Sarc, F. Kapor, *Materials and Corrosion* 53 (2002) 266.
20. E. Almeida, D. Pereira, M.O Figueiredo, V.M.M Lobo, M. Morcillo, *Corros. Sci*. 39(9) (1997) 1567.
21. J. Aroma, A. Klarin, Materials, Corrosion Prevention, and Maintenance. Finland: Fapet Oy, 1999.
22. M. J. Bahrami, S. M. A. Hosseini, P. Pilvar, *Corros. Sci*. 52 (2010) 2795.
23. I. Ahamad, R. Prasad, M.A. Quraishi, *Corros. Sci*. 52 (2010) 1474–1475.

24. V.S. Sastri, E. Ghali, M. Elboujdaini, Corrosion Prevention and Protection: Practical Solutions, John Wiley & Sons Ltd., New Jersey, 2007.
25. A.M. Abdel-Gaber, B. A. Abd-El-Nabey, I. M. Sidahmed, A. M. El-Zayady, M. Saadawy, *Corros. Sci*. 48 (2006) 2765.
26. J. R. Macdonald, W. B. Johanson, in: J. R. Macdonald (Ed.), Theory in Impedance Spectroscopy, John Wiley & Sons Ltd., New Jersey, 1987.
27. M. S. Abdelaal, M. S. Morad, *Br. Corros. J*. 36 (2001) 253.
28. P. Bommersbach, C. Alemany-Dumont, J.P. Millet, B. Normand, *Electrochim. Acta* 51 (2005) 1076.
29. F. Mansfeld, Corrosion 36 (1981) 301; F. Mansfeld, *Corrosion* 38 (1982) 570.
30. A.V. Benedetti, P. T .A. Sumodjo, K. Nobe, P. L. Cabot, W. G. Proud, *Electrochim. Acta* 40 (1995) 2657.
31. A. Popova, E. Sokolova, S. Raicheva, M. Christov, *Corros. Sci*. 45 (2003) 33.
32. F. S. de Souza, A. Spinelli, *Corros. Sci*. 51 (3) (2009) 646
33. M. Bouklah, N. Benchat, B. Hammouti, A. Aouniti, S. Kertit, *Mater. Lett.* 60 (2006) 1904.
34. K. O. Orubite, N. C. Oforka, *Mater. Lett*. 58 (2004) 1772.
35. D. Wahyuningrum, S. Achmad, Y.M. Syah, Buchari, B. Bundjali, B. Ariwahjoedi, *Int. J. Electrochem. Sci*. 3 (2008) 164.
36. M.S. Morad, A.M. Kamal El-Dean, *Corros. Sci*. 48 (2006) 3409.
37. S. Cheng, S. Chen, T. Liu, X. Chang, Y. Yin, *Mater. Lett*. 61 (2007) 3279.
38. F.M. Donahue, K. Nobe, *J. Electrochem. Soc*. 112 (1965) 886.
39. E. Kamis, F. Bellucci, R.M. Latanision, E.S.H. El-r, *Corrosion* 47 (1991) 677.
40. H.H. Hassan, E. Abdelghani, M.A. Amin. *Electrochim. Acta* 52 (2007) 6362–6364.
41. R. Solmaz, G. Kardas, B. Yazici, M. Erbil. Colloid and Surfaces A: Physicochemical Engineering Aspects 312 (2008) 15-16.
42. H. Keles, M. Keles, I. Dehri, O. Serindag. Colloid and Surfaces A: Physicochemical Engineering Aspects 320 (2008), 142-143.
43. M.A. Amin, S.S. Abd El-Rehim, E.E.F. El-Sherbini, R. S. Bayoumi, *Electrochim. Acta* 52 (2007) 3588–3600.
44. M.H. Hussin, Uncaria gambir as natural corrosion inhibitor for mild steel in acidic solution, Master's Thesis, Universiti Sains Malaysia, Penang, 2010.